Mineralogy and Petrology (2004) 82: 137–156
DOI 10.1007/s00710-004-0049-1

Mineralogy and Petrology
Printed in Austria

Palladium and gold minerals from the Baronskoe-Kluevsky ore deposit (Volkovsky complex, Central Urals, Russia)

F. Zaccarini[1], **E. Anikina**[2], **E. Pusharev**[2], **I. Rusin**[2], and **G. Garuti**[3]

[1] Department of Applied Geosciences and Geophysics, University of Leoben, Austria
[2] Institute of Geology and Geochemistry, Ural-branch of the Russian Academy of Sciences, Ekaterinburg, Russia
[3] Department of Earth Sciences, University of Modena and Reggio Emilia, Modena, Itlay

Received April 2, 2004; revised version accepted May 10, 2004
Published online July 20, 2004;
Editorial handling: *E. F. Stumpfl* and *J. G. Raith*

Summary

Drill cores from the newly discovered Baronskoe-Kluevsky Pd–Au deposit (Volkovsky massif, Central Urals) have been investigated by reflected-light and electron microscopy, and the ore minerals were analyzed by electron microprobe. The most abundant Platinum-group mineral (PGM) is vysotskite, ideally PdS, characterized by an unusual Pt,Ni-poor composition. Palladium also occurs in kotulskite (PdTe), stillwaterite (Pd_8As_3), and unknown Pd–As–Te compounds with vincentite-type $Pd_3(As,Te)$, stillwaterite-type $Pd_8(As,Te)_3$, and $Pd_7(As,Te)_2$ stoichiometries. The main carrier of Au is Pd-rich electrum, approaching the composition $Au_{75}Ag_{15}Pd_{10}$, with minor Fe, Cu, Ni and Pt. The precious minerals are closely associated with minute blebs of chalcopyrite + magnetite disseminated throughout serpentinized olivine-apatite host rock. Paragenetic relationships among the ore minerals define a succession of crystallization events in the order: 1) Cu–Pd sulfides + electrum, 2) replacement by Pd–Te–As and late Pd–As PGM, 3) final replacement by magnetite. The paragenesis is tentatively related with cooling of a fluid phase in the late- to post-magmatic stage.

Introduction

The discovery of ''new types'' and ''unconventional'' Platinum-group elements (PGE) mineralization in the so-called ''Platinum-bearing Belt'' of the Urals has been emphasized in the recent literature (*Volchenko* and *Koroteev*, 1998; *Anderson*

and *Martineau*, 2002). Some deposits, defined as the Kachkanar-type and Volkovsky-type (*Volchenko* et al., 1975; *Murzin* et al., 1988; *Volchenko* and *Koroteev*, 1998), are characterized by a Au–Ag–Pd–(Pt) assemblage and occur in gabbroic rocks, bearing spatial, but not necessarily genetic, relationships with the Ural-Alaskan type complexes, characterized by the dunite-hosted chromite-Pt ores. Among these deposits, the Pd–Au mineralization associated with Cu-sulfide ores in the lower layered section of the Volkovsky gabbro massif is the most unusual. There, drilling has located two potentially economic ore bodies at the localities of Baranskoe and Kluevsky. Preliminary geochemical data indicate that the ore contains 6.4–15.7 g/t Pd, 0.5–7 g/t Au, and less than 0.4 g/t Pt (*Zoloev* et al., 2001; *Anderson* and *Martineau*, 2002). The Pd–Au mineralization was initially interpreted as to be magmatic in origin. However, the observation that high-grade ore is locally associated with shear zones, led to an alternative model involving the action of hydrothermal fluids (*Anderson* and *Martineau*, 2002, and references therein).

This work reports the results of a detailed mineralogical investigation of selected mineralized samples from the Baranskoe-Kluevsky deposit. The reflected-light and electron microscope study of polished sections, as well as the electron microprobe quantitative analysis of the ore minerals, has revealed a complex Pd–Au mineralogy. The texture of the ore minerals has been studied in detail with BSE electron microscopy in order to understand their order of crystallization and paragenetic relationships.

Geological background

The Volkovsky complex is located in the southern part of the Ural Platinum Belt (UPB), between the Main Uralian and Serov-Mauk faults, about 45 km N of the Nizny Tagil Uralian-Alaskan type dunite–clinopyroxenite intrusion (Fig. 1). The complex pertains to the Tagil-Barancha gabbro–diorite–syenite complex (*Ivanov*, 1997), and is in contact with volcanic and sedimentary rocks of the Tagil Island-Arc Zone, to the east, and with metabasaltic hornfels (''kytlyimite''), to the west (Fig. 2). The Volkovsky complex consists of gabbro and minor ultramafic rocks intruded by diorites and syenites. The ultramafic rocks occur in two NW–SE elongated bodies (Baranskoe and Kluevsky) in the southern part of the massif. They consist of olivine-rich rock (in Russian literature called olivinite), wehrlite, clinopyroxenite, plagioclase clinopyroxenite and olivine gabbro that frequently contain substantial amounts of Ti-rich magnetite, amphibole, apatite, with accessory phlogopite and disseminated sulfides (mainly pyrite, chalcopyrite and bornite) up to 0.5% by volume. The field relations are not well exposed, and were established mainly from drilling and trenching carried out during exploration. Structural observations indicate poor stratigraphic correlation among the bore holes. The various rocks define an irregular succession of lenses and discontinuous layers trending about NW–SE and dipping 60°–70° NE, although the dip-angle can vary widely as a result of tectonic displacement. Effects of tectonic overprint are widespread, thereby the rocks were locally brecciated and saussuritized with strong serpentine–talc–tremolite, chlorite–titanite and epidote–carbonate–scapolite alteration.

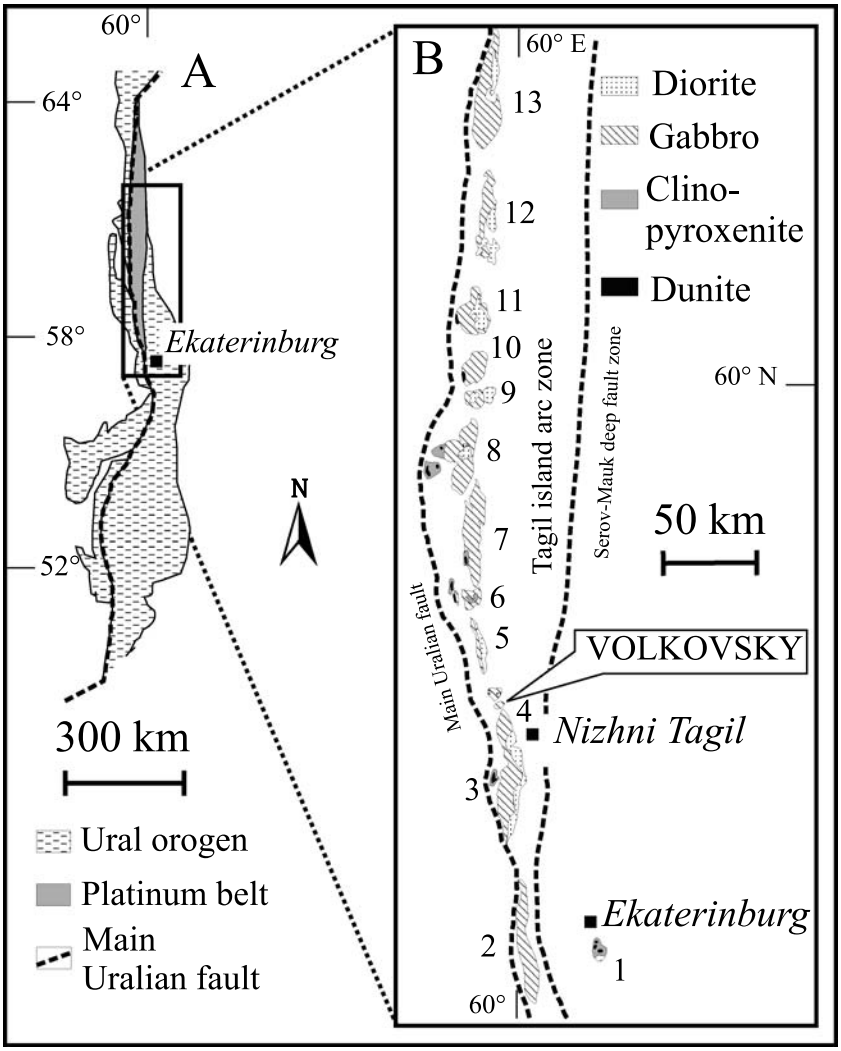

Fig. 1. **A** Location of the ''Ural Platinum Belt'' in the Ural orogen, and **B** geological setting of the Volkovksy gabbro complex in relation to the major Ural-Alaskan-type complexes of the Ural Platinum Belt; 1 = Uktus, 2 = Revda, 3 = Tagil, 4 = Tagil-Barancha, 5 = Arbat, 6 = Kachkanar, 7 = Pavda, 8 = Kytlym, 9 = Knyaspin, 10 = Kumba, 11 = Denezhk, 12 = Pomursk, 13 = Chistop (modified after *Yefimov* et al., 1993)

The Pd–Au mineralization occurs inside the ultramafic suite. Initial exploration by soil geochemistry revealed Pd–Au anomalies extending over an area about 10 meters wide and 900 meters long (*Potter*, 2002). A subsequent soil geochemistry survey indicated that the anomaly is even more extended at Kluevsky covering an area of 100×1300 m (*Anderson* and *Martineau*, 2002). Drilling has intersected the mineralization in a zone of transition from layered olivinite, wehrlite and olivine–clinopyroxenite to olivine-free, plagioclase-bearing clinopyroxenite, grading into gabbros upward. The ore bodies occur predominantly in olivine-rich rocks (mainly apatite–olivinite) and, to a minor extent, in plagioclase pyroxenite (*Anderson* and *Martineau*, 2002).

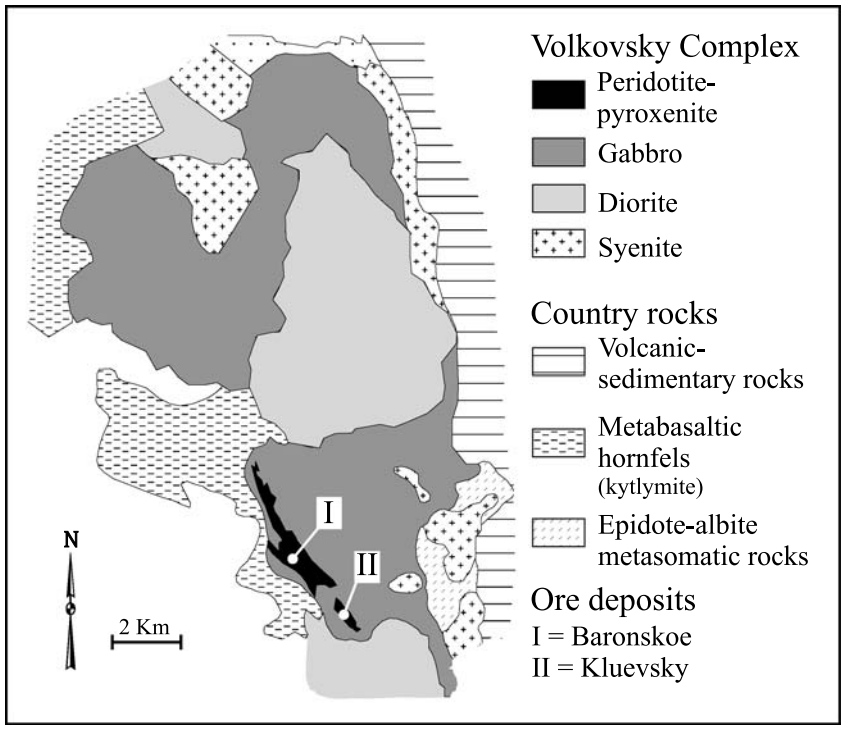

Fig. 2. Geological sketch map of the Volkovksy complex and location of the Pd–Au Baronskoe-Kluevskoy deposits

Description of the investigated samples

The polished sections examined in this study were obtained from drill cores in the Kluevsky ore body. Drilling to a depth of 100 meters revealed a transition from an upper part consisting of olivine-free, plagioclase-rich pyroxenite layers, with minor gabbro and plagioclasite, to a lower part of dominant olivine-bearing rocks, mainly olivine–pyroxenite and wehrlite with minor olivinite and apatite-rich plagioclase olivinite (Fig. 3). With a few exceptions, all rocks contain hornblende and Ti-rich magnetite. Sulfides are more abundant in the lower ultramafic rocks having up to 0.25 wt% S, that is mainly accounted for by disseminated pyrite and chalcopyrite. The Pd and Au anomalies have been observed at several stratigraphic intervals along the cross section; they show no obvious correlation with the distribution of sulfides. The highest Pd concentrations occur in olivine-rich rocks (olivine pyroxenite, wehrlite and olivinite), and in particular in one 30 cm-thick horizon of serpentinized olivinite, containing over 10 ppm Pd, 130–314 ppm Cu, and 0.02–0.04 wt% S. This mineralized rock consists of 8–10 modal% apatite, along with 7–10% saussuritized plagioclase, accessory phlogopite, amphibole, and secondary chlorite. Several tens of PGM grains were encountered in the examined samples. They typically occur associated with interstitial patches (50 to 300 μm) of chalcopyrite, disseminated unevenly in the host rock, where plagioclase and phlogopite are less abundant. Chalcopyrite is accompanied by minor bornite, carrollite

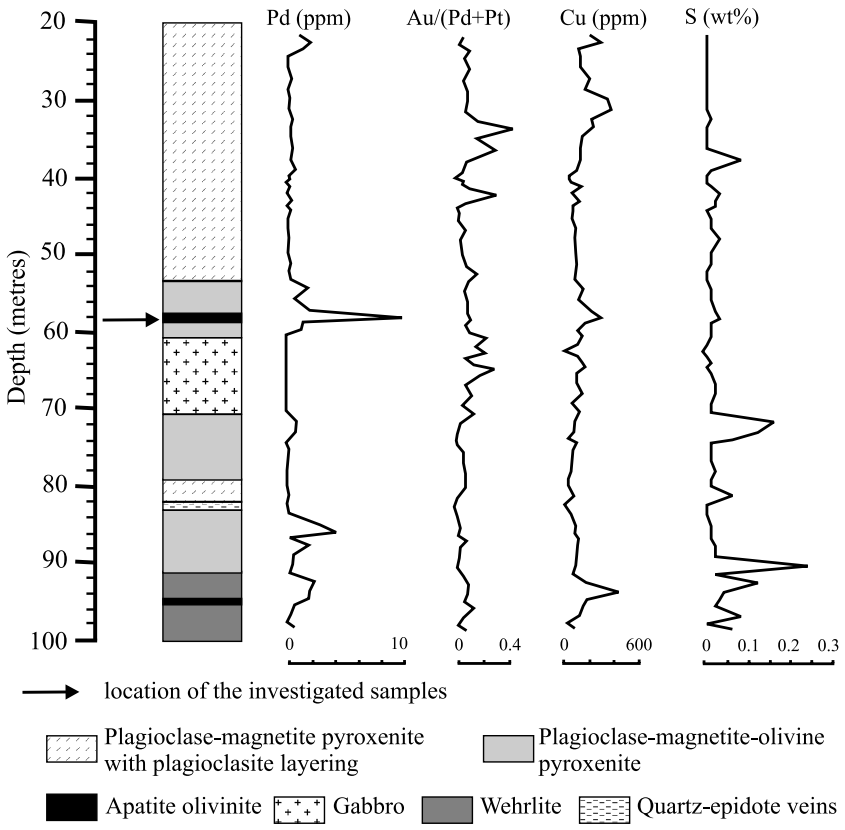

Fig. 3. Location of the investigated samples in the stratigraphy of the Kluevsky bore hole, and variation of relevant geochemical parameters (redrawn from the *Year Book 2003* of the Institute of Geology and Geochemistry, Ural-branch of the Russian Academy of Sciences)

$Cu(Co,Ni)_2S_4$, and native copper. Pyrite was not observed. The sulfide blebs are systematically rimmed or almost completely replaced by pseudomorphic magnetite, leaving only a few small relics of chalcopyrite, PGM and gold immersed in the Fe-oxide mass. This magnetite is Ti-free and also occurs as filling in fissures and cracks with the silicate matrix. Therefore it differs from the interstitial grains of Ti-rich magnetite disseminated in the gabbro-pyroxenite rocks of the Volkovsky complex.

Analytical notes

The PGM and Au minerals were located on polished sections using reflected-light microscopy at 250–800× magnification. They were investigated in-situ using electron microscopy and microprobe techniques. Back scattered electron (BSE) images were obtained at the Inter-Department Instrumental Center (CIGS) of the University of Modena, using a Philips XL40 electronic microscope operated at 15–20 kV and 20 nA. The electron microprobe analyses were performed at the Department of Earth Sciences, University of Modena, using an ARL-SEMQ instrument equipped with both EDS and WDS analyzers and operated at 20–27 kV accelerating voltage

and 10–20 nA beam current, with a beam diameter of about 1 μm. Counting times of 20 and 5 seconds were used for peak and backgrounds, respectively. The X-ray Kα lines were used for S, Fe, Ni, and Cu; Lα lines for Rh, Pt, Pd, Ag, As, Te, and Sb and the Mα line for Au. Pure metals were used as standards for Pt and Rh, and synthetic $Au_{70}Ag_{30}$, PdTe, Sb_3S_2, NiAs, FeS_2 and $CuFeS_2$ for Au, Ag, Pd, Te, Sb, Ni, Fe, Cu, S, and As. Correction for the interferences Ru–Rh, and Rh–Pd, and detection limit calculation for PGE were automatically performed with the updated version 3.63, January 1996, of the PROBE software (*Donovan* and *Rivers*, 1990). The average detection limits (wt%) for the analyzed elements were: Au = 0.35, Ag = 0.09, Pd = 0.52, Pt = 0.30, Rh = 0.08, Fe = 0.05, Ni = 0.05, Cu = 0.07, Te = 0.06, S = 0.03, As = 0.16 and Sb = 0.50.

The palladium and gold minerals

The Pd and Au minerals are usually associated with chalcopyrite–magnetite blebs in extremely variable proportions, showing a prevalence of the precious minerals in some cases. The precious mineral assemblage mainly consists of vysotskite accompanied by kotulskite, stillwaterite, a group of unknown Pd–As–Te minerals and electrum. One small grain (<2 μm) of Pt-bearing Cu sulfide, associated with chalcopyrite, was encountered, but could be analyzed only qualitatively because its small size. The optical and electronic properties, as well as morphology and textural relations of the PGM and Au are illustrated in Figs. 4 to 6, while the results of the electron microprobe analyses are listed in Tables 1 to 3, and shown in Figs. 7 and 8.

Vysotskite

Vysotskite is the most abundant Pd-mineral encountered in the Baranskoe-Kluevsky samples. Under the reflected-light microscope, vysotskite shows weak to distinct anisotropy. It appears creamy white or bluish white in color depending on the minerals in contact, chalcopyrite and magnetite (Fig. 4A, B) or Pd–As–Te PGM's (Fig. 4C). In agreement with the observations by *Criddle* and *Stanley* (1985), reflectance of vysotskite in the Baranskoe-Kluevsky samples appears slightly higher than that of chalcopyrite, but is remarkably lower than that of the other Pd–PGM. In BSE images, vysotskite has intermediate electronic reflectance between chalcopyrite and the associated Pd–As–Te PGM's (Fig. 4C-1). Vysotskite usually occurs at the core of the blebs surrounded by chalcopyrite (Fig. 4A, B), which is almost completely replaced by magnetite in the most advanced altered samples (Fig. 5A–C). The grain contacts between the two phases are generally smooth and rounded, although reciprocal inclusions chalcopyrite–vysotskite or more complex graphic intergrowths have also been observed (Fig. 6A–C). Vysotskite may contain small inclusions of kotulskite and electrum, that are likely to be exsolution products (Figs. 4C, 5B, C). Vysotskite is replaced along the grain boundaries by stillwaterite and the other Pd–As–Te PGM's (Figs. 4C, 5D).

Electron microprobe analyses (Table 1) show minor content of Ni (0.07–3.95 wt%), Ag (<1.1 wt%), and Pt (<1.0 wt%) with only two grains having Pt contents of up to 4.76 and 14.93 wt%, respectively. Minor amounts of Fe (<1.35 wt%)

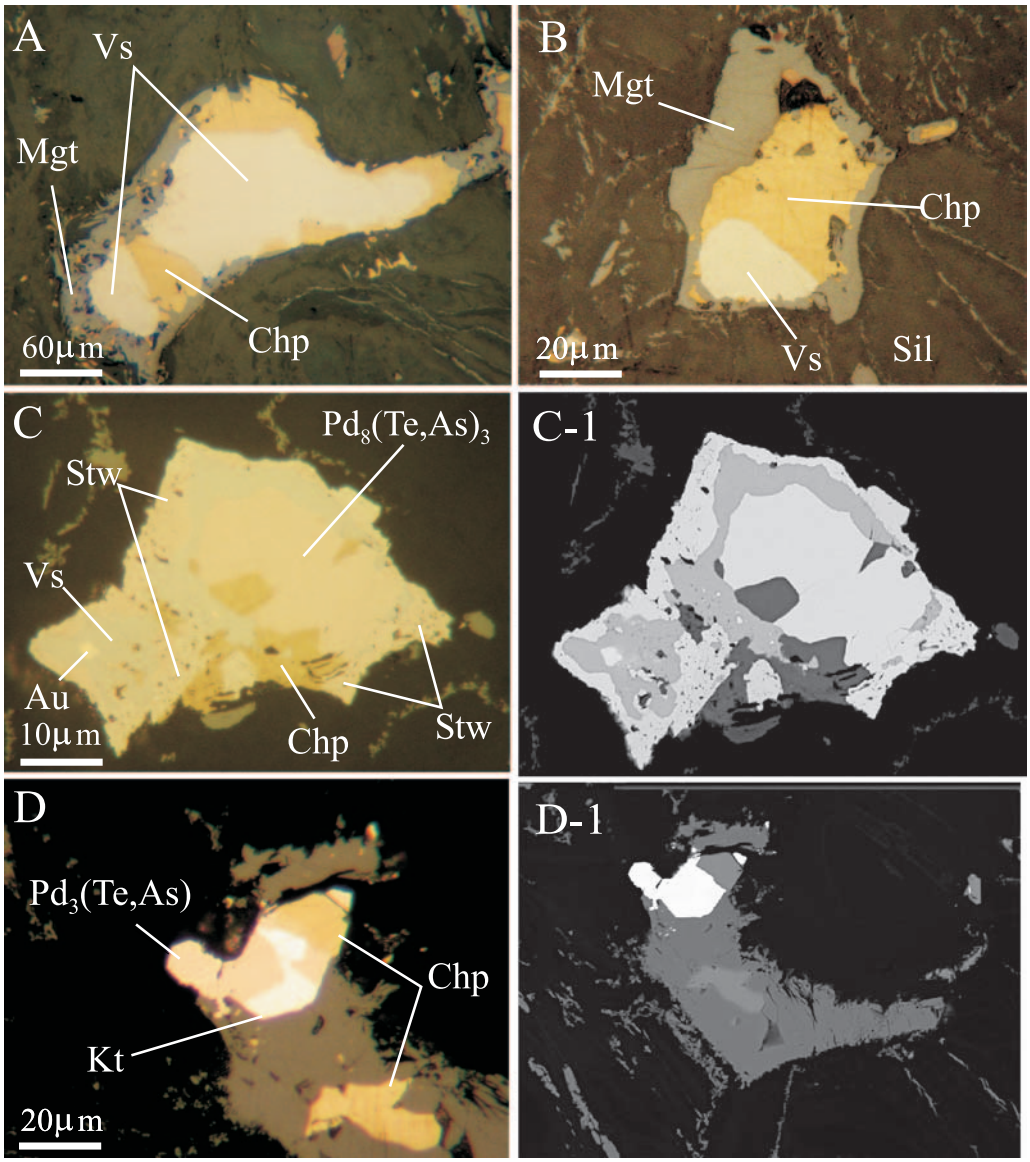

Fig. 4. Reflected light and BSE images showing textural relations and comparison of optical and electronic properties of Pd–PGM from Kluevsky. **A**, **B** Different types of vysotskite–chalcopyrite textural association. Note the minute magnetite veins in the silicate matrix. **C**, **C-1** Vysotskite, chalcopyrite replaced by $Pd_8(Te,As)_3$ that is replaced in its turn by stillwaterite. **D**, **D-1** Vincentite–kotulskite association at the margin of a chalcopyrite bleb almost totally replaced by magnetite. *Vs* vysotskite, *Chp* chalcopyrite, *Mgt* magnetite, *Stw* stillwaterite, *$Pd_8(Te,As)_3$* Te-rich stillwaterite (?), *Au* Electrum, *Kt* kotulskite, *$Pd_3(Te,As)$* Te-rich vincentite (?), *Sil* silicate matrix

and Cu (<0.45 wt%) were detected in some grains. The plot of vysotskite compositions in the Pd–Pt–Ni ternary diagram (Fig. 7) indicates very limited solid solution of vysotskite with braggite and millerite. This appears to be a distinctive feature of

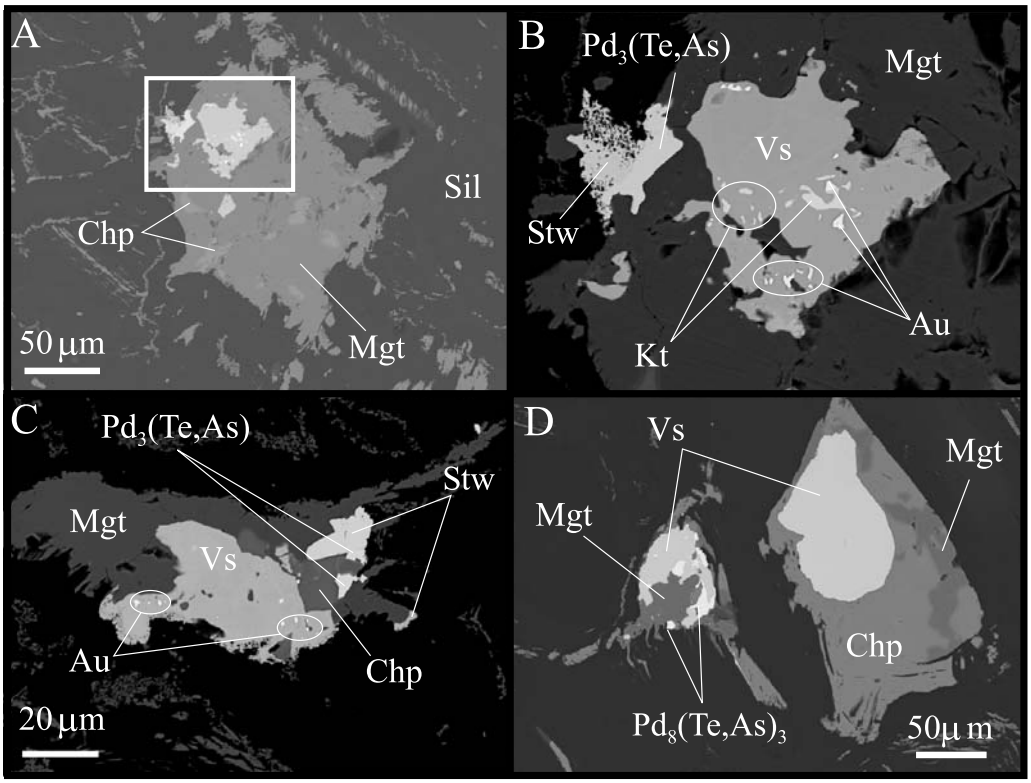

Fig. 5. BSE images of Pd–PGM from Kluevsky. **A** Chalcopyrite bleb replaced by magnetite, with vysotskite (included) and Te-rich vincentite (?) + stillwaterite at the rim; **B** Enlarged field: kotulskite + electrum exsolution in vysotskite, porous stillwaterite replacing Te-rich vincentite (?). **C** Electrum exsolution in vysotskite; Te-rich vincentite (?) and stillwaterite at the rim of the bleb. **D** Vysotskite–chalcopyrite blebs with Te-rich stillwaterite (?) replacing vysotskite. Labels as in Fig. 4

the Baranskoe-Kluevsky samples compared with vysotskite from other localities worldwide. In particular it differs from the vysotskite of Noril'sk, where it was reported for the first time (*Genkin* and *Zvyagintsev*, 1962), and vysotskite documented in other PGE deposits such as Bushveld (*Verryn* and *Merkle*, 1994), Stillwater (*Cabri* and *Laflamme*, 1974; *Cabri* et al., 1978; *Todd* et al., 1982; *Volborth* et al., 1986), Lac des Isles (*Cabri* and *Laflamme*, 1974), Monchetundra (*Grokhovkaya* et al., 2002), Penikat (*Halkoaho*, 1989; *Barkov* et al., 2002) and Sierra Leone (*Bowles*, 2000).

Kotulskite

Kotulskite was recognized under the optical microscope because of its white color, distinct anisotropy, and high reflectance (Fig. 4D). In BSE images it is very similar to the other Pd PGM's (Fig. 4D-1) and therefore it cannot be identified in BSE images. Kotulskite generally occurs as relatively large patches ($\sim 15 \times 20\,\mu m$) intimately intergrown with the unknown $Pd_3(As,Te)$ phase, the texture suggesting

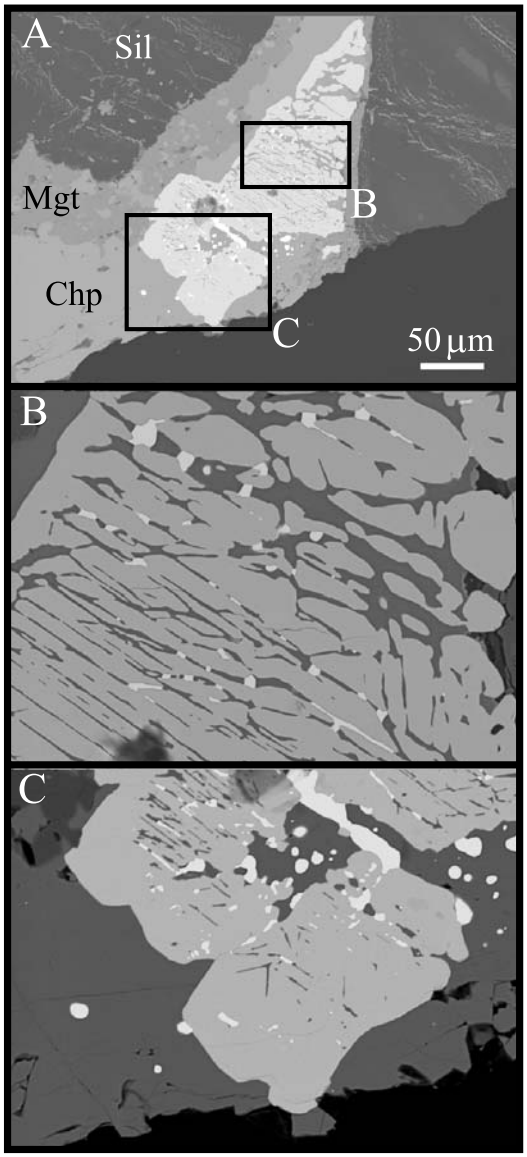

Fig. 6. BSE images of the graphic intergrowth among vysotskite, chalcopyrite and electrum. Labels as in Fig. 4

co-crystallization of the two phases. However, it has also been observed as exsolution blebs and lamellae (<5 μm) within vysotskite grains (Fig. 5B). The latter paragenesis also includes electrum suggesting that it formed by equilibration of a homogeneous Pd–S–Te–Au phase. Electron microprobe analyses indicate that the two kotulskite types have similar composition, corresponding to PdTe, with slight deficiency in Te (Fig. 8).

Stillwaterite

Stillwaterite was not readily recognized by observation in reflected light because it has optical properties (creamy-pinkish color, weak anisotropy and reflectance)

Table 1. *Representative microprobe analyses of vysotskite, kotulskite and stillwaterite from Baronskoe-Kluevsky*

Weight %	Au	Ag	Pd	Pt	Rh	Fe	Ni	Cu	Te	S	As	Sb	Totals
Vysotskite (Pd,Pt,Ni)S													
Vs 1	0.00	0.00	73.39	0.22	0.00	0.04	0.09	0.12	0.00	23.08	0.00	0.00	96.95
Vs 2	0.00	0.72	71.01	0.90	0.00	0.24	0.21	0.19	0.03	24.52	0.00	0.35	98.16
Vs 3	0.16	1.09	70.98	0.37	0.00	1.36	0.87	0.26	0.04	25.45	0.00	0.00	100.56
Vs 4	0.00	0.00	73.80	0.00	0.00	0.79	0.64	0.17	0.00	24.35	0.00	0.00	99.75
Vs 5	0.13	0.00	74.74	0.00	0.00	0.69	0.44	0.05	0.00	24.63	0.00	0.00	100.68
Vs 6	0.00	0.00	74.21	1.15	0.00	0.18	0.56	0.12	0.00	23.68	0.00	0.00	99.89
Vs 7	0.00	0.00	59.18	14.93	0.06	0.15	2.23	0.06	0.00	21.97	0.00	0.00	98.58
Vs 8	0.00	0.33	72.23	0.16	0.00	0.56	0.34	0.06	0.00	23.42	0.00	0.00	97.10
Vs 9	0.23	0.00	71.89	0.98	0.00	0.52	0.63	0.09	0.00	22.63	0.00	0.00	96.96
Kotulskite PdTe													
Kt 1	0.00	0.00	45.62	0.00	0.00	0.94	0.00	0.09	54.75	0.00	0.00	0.00	101.41
Kt 2	0.00	0.00	45.90	0.00	0.00	1.53	0.03	0.06	54.35	0.00	0.00	0.00	101.87
Stillwaterite Pd_8As_3													
Stw 1	0.00	1.73	73.70	0.00	0.00	1.26	0.00	0.19	0.03	0.02	20.53	0.00	97.45
Stw 2	0.17	1.04	73.99	0.08	0.04	1.39	0.04	0.22	0.00	0.00	20.56	0.00	97.52
Stw 3	0.00	0.00	74.65	0.55	0.00	1.22	0.00	0.02	0.06	0.02	20.44	0.15	97.10
Stw 4	0.00	1.47	77.10	1.06	0.00	0.32	0.03	0.35	0.02	0.15	21.10	0.00	101.60
Stw 5	0.00	0.00	76.61	0.00	0.00	0.89	0.06	0.37	0.01	0.02	21.18	0.00	99.14

(*continued*)

Table 1 (*continued*)

Atomic %	Au	Ag	Pd	Pt	Rh	Fe	Ni	Cu	Te	S	As	Sb
Vysotskite (Pd,Pt,Ni)S												
Vs 1	0.00	0.00	48.75	0.08	0.00	0.05	0.11	0.14	0.00	50.87	0.00	0.00
Vs 2	0.00	0.46	45.80	0.32	0.00	0.29	0.25	0.20	0.02	52.47	0.00	0.20
Vs 3	0.05	0.66	43.98	0.12	0.00	1.60	0.97	0.27	0.02	52.31	0.00	0.00
Vs 4	0.00	0.00	46.84	0.00	0.00	0.96	0.74	0.18	0.00	51.28	0.00	0.00
Vs 5	0.04	0.00	47.08	0.00	0.00	0.83	0.50	0.05	0.00	51.49	0.00	0.00
Vs 6	0.00	0.00	47.90	0.40	0.00	0.22	0.65	0.13	0.00	50.70	0.00	0.00
Vs 7	0.00	0.00	40.90	5.63	0.04	0.20	2.80	0.06	0.00	50.37	0.00	0.00
Vs 8	0.00	0.22	47.48	0.06	0.00	0.70	0.40	0.07	0.00	51.08	0.00	0.00
Vs 9	0.08	0.00	47.95	0.35	0.00	0.66	0.76	0.10	0.00	50.09	0.00	0.00
Kotulskite PdTe												
Kt 1	0.00	0.00	48.93	0.00	0.00	1.93	0.01	0.17	48.97	0.00	0.00	0.00
Kt 2	0.00	0.00	48.68	0.00	0.00	3.09	0.05	0.11	48.06	0.00	0.00	0.00
Stillwaterite Pd_8As_3												
Stw 1	0.00	1.59	68.66	0.00	0.00	2.23	0.00	0.29	0.03	0.06	27.16	0.00
Stw 2	0.08	0.95	68.84	0.04	0.03	2.46	0.07	0.34	0.00	0.00	27.17	0.00
Stw 3	0.00	0.00	70.06	0.28	0.00	2.18	0.00	0.03	0.04	0.05	27.24	0.12
Stw 4	0.00	1.31	69.55	0.52	0.00	0.54	0.05	0.53	0.02	0.45	27.03	0.00
Stw 5	0.00	0.00	70.16	0.00	0.00	1.56	0.10	0.57	0.00	0.06	27.54	0.00

Table 2. *Representative microprobe analyses of unknown Pd–Te–As minerals from Baronskoe-Kluevsky*

Weight %	Au	Ag	Pd	Pt	Rh	Fe	Ni	Cu	Te	S	As	Sb	Totals
Unknown $Pd_8(Te,As)_3$, possibly Te-rich stillwaterite													
Te-stw 1	0.14	0.24	71.64	0.00	0.00	0.37	0.00	0.41	16.03	0.04	9.79	0.00	98.66
Te-stw 2	0.00	0.00	71.23	0.53	0.05	0.99	0.04	1.08	16.46	0.11	9.83	0.00	100.34
Te-stw 3	0.00	0.00	70.84	0.13	0.00	1.36	0.00	0.04	15.78	0.06	10.17	0.00	98.39
Te-stw 4	0.00	0.00	70.45	0.00	0.00	1.10	0.00	0.15	15.75	0.05	9.70	0.00	97.19
Te-stw 5	0.00	0.73	71.89	0.00	0.00	0.69	0.00	0.74	16.72	0.04	10.15	0.00	100.98
Te-stw 6	0.00	0.56	72.59	0.00	0.00	0.41	0.00	0.58	16.85	0.03	10.02	0.00	101.04
Te-stw 7	0.00	1.49	70.65	0.00	0.00	0.07	0.08	0.11	15.72	0.00	9.98	0.00	98.10
Te-stw 8	0.00	0.00	72.51	0.13	0.00	0.15	0.05	0.04	15.55	0.11	9.92	0.00	98.46
Te-stw 9	0.00	0.00	71.68	0.13	0.00	0.37	0.03	0.03	16.04	0.00	9.93	0.00	98.20
Te-stw 10	0.00	1.16	70.97	0.00	0.00	0.08	0.05	0.06	15.98	0.00	9.72	0.00	98.03
Te-stw 11	0.00	1.97	69.34	0.00	0.00	0.09	0.04	0.15	16.09	0.00	9.61	0.00	97.30
Te-stw 12	0.19	0.00	72.16	0.00	0.00	0.15	0.06	0.09	16.23	0.00	9.87	0.00	98.76
Unknown $Pd_3(Te,As)$, possibly Te-rich vincentite													
Te-vin 1	0.00	0.00	73.66	0.00	0.00	0.55	0.02	0.09	14.67	0.00	9.21	0.00	98.20
Te-vin 2	0.13	0.00	73.53	0.19	0.00	0.78	0.00	0.06	13.48	0.00	9.58	0.21	97.96
Te-vin 3	0.00	0.00	76.15	0.00	0.00	0.51	0.00	0.00	14.03	0.00	9.61	0.00	100.30
Te-vin 4	0.00	0.00	75.25	0.00	0.00	0.67	0.00	0.05	14.53	0.00	9.59	0.00	100.09
Madagascar*			63.85	12.79		1.25		0.60	13.74	0.46	5.58		98.27
Ecuador**			74.61	2.02				0.64	14.57		9.17		101.01
Unknown $Pd_7(Te,As)_2$													
Un. 1	0.00	0.00	75.32	0.00	0.03	0.36	0.00	0.55	12.02	0.03	9.02	0.00	97.32
Un. 2	0.00	0.00	76.59	0.00	0.00	0.44	0.02	0.63	11.65	0.03	9.24	0.00	98.60
Unknown $Pd_9(Te,As)_4$													
Un. 3	0.00	0.00	70.34	0.00	0.00	0.47	0.00	0.14	22.02	0.00	8.99	0.00	101.95
Un. 4	0.00	0.00	71.21	0.68	0.00	0.95	0.06	0.53	16.01	0.91	9.41	0.00	99.76

(*continued*)

Table 2 (*continued*)

Atomic %	Au	Ag	Pd	Pt	Rh	Fe	Ni	Cu	Te	S	As	Sb
Unknown $Pd_8(Te,As)_3$, possibly Te-rich stillwaterite												
Te-stw 1	0.07	0.24	71.10	0.00	0.00	0.69	0.00	0.69	13.26	0.14	13.80	0.00
Te-stw 2	0.00	0.00	68.89	0.28	0.05	1.83	0.07	1.75	13.27	0.35	13.50	0.00
Te-stw 3	0.00	0.00	69.86	0.07	0.00	2.56	0.00	0.07	12.98	0.21	14.25	0.00
Te-stw 4	0.00	0.00	70.56	0.00	0.00	2.09	0.00	0.25	13.15	0.16	13.79	0.00
Te-stw 5	0.00	0.70	69.34	0.00	0.00	1.27	0.00	1.20	13.45	0.14	13.90	0.00
Te-stw 6	0.00	0.53	70.30	0.00	0.00	0.75	0.00	0.94	13.61	0.09	13.78	0.00
Te-stw 7	0.00	1.47	70.75	0.00	0.00	0.13	0.14	0.18	13.12	0.00	14.20	0.00
Te-stw 8	0.00	0.00	72.19	0.07	0.00	0.28	0.10	0.07	12.90	0.37	14.02	0.00
Te-stw 9	0.00	0.00	71.66	0.07	0.00	0.70	0.05	0.06	13.37	0.00	14.09	0.00
Te-stw 10	0.00	1.15	71.26	0.00	0.00	0.16	0.09	0.09	13.38	0.00	13.87	0.00
Te-stw 11	0.00	1.97	70.14	0.00	0.00	0.18	0.08	0.26	13.57	0.00	13.81	0.00
Te-stw 12	0.10	0.00	71.90	0.00	0.00	0.29	0.11	0.15	13.48	0.00	13.97	0.00
Unknown $Pd_3(Te,As)$, possibly Te-rich vincentite												
Te-vin 1	0.00	0.00	73.51	0.00	0.00	1.04	0.03	0.15	12.21	0.00	13.06	0.00
Te-vin 2	0.07	0.00	73.29	0.11	0.00	1.48	0.00	0.10	11.20	0.00	13.57	0.18
Te-vin 3	0.00	0.00	74.31	0.00	0.00	0.94	0.00	0.00	11.42	0.00	13.32	0.00
Te-vin 4	0.00	0.00	73.52	0.00	0.00	1.25	0.00	0.08	11.84	0.00	13.31	0.00
Madagascar*	0.00	0.00	67.13	7.33	0.00	2.50	0.00	1.06	12.04	1.60	8.33	0.00
Ecuador**	0.00	0.00	73.18	1.08	0.00	0.00	0.00	1.05	11.92	0.00	12.77	0.00
Unknown $Pd_7(Te,As)_2$												
Un. 1	0.00	0.00	75.41	0.00	0.03	0.69	0.00	0.92	10.03	0.10	12.82	0.00
Un. 2	0.00	0.00	75.49	0.00	0.00	0.82	0.04	1.04	9.58	0.09	12.94	0.00
Unknown $Pd_9(Te,As)_4$												
Un. 3	0.00	0.00	68.57	0.00	0.00	0.87	0.00	0.23	17.89	0.00	12.44	0.00
Un. 4	0.00	0.00	68.40	0.35	0.00	1.73	0.10	0.86	12.82	2.89	12.83	0.00

* *Augé* and *Legendre* (1992), ** *Weiser* and *Schimdt-Thomé* (1993)

Table 3. *Representative microprobe analyses of electrum from Baronskoe-Kluevsky*

Weight %	Au	Ag	Pd	Pt	Fe	Ni	Cu	Te	S	Totals
Au 1	82.53	8.27	6.02	0.19	0.51	0.06	1.89	0.02	0.42	99.90
Au 2	82.07	9.15	4.37	0.23	1.73	0.08	0.50	0.02	0.10	98.25
Au 3	81.79	8.35	6.79	0.31	0.18	0.04	0.63	0.04	0.07	98.18
Au 4	85.63	6.74	5.67	0.18	2.40	0.03	0.45	0.03	0.03	101.16
Au 5	85.42	6.50	5.42	1.15	0.63	0.18	0.29	0.05	0.12	99.76
Au 6	84.32	7.98	7.04	0.28	0.18	0.01	0.30	0.01	0.02	100.13
Au 7	84.27	8.47	6.92	0.02	0.06	0.01	0.23	0.00	0.00	99.97
Au 8	84.42	8.20	7.39	0.04	0.02	0.02	0.20	0.04	0.01	100.33
Au 9	85.81	9.51	4.91	0.31	0.70	0.06	0.55	0.03	0.03	101.90
Au 10	84.55	8.82	5.55	0.00	0.77	0.00	1.07	0.00	0.03	100.78
Au 11	82.24	10.36	4.55	0.03	0.71	0.25	0.75	0.02	0.11	99.03
Au 12	84.31	9.62	5.81	0.16	0.14	0.04	0.41	0.01	0.02	100.51
Atomic %	Au	Ag	Pd	Pt	Fe	Ni	Cu	Te	S	
Au 1	69.10	12.65	9.33	0.16	1.51	0.16	4.91	0.02	2.16	
Au 2	70.97	14.45	7.00	0.21	5.29	0.22	1.33	0.03	0.52	
Au 3	72.32	13.48	11.11	0.28	0.55	0.13	1.73	0.06	0.35	
Au 4	72.10	10.36	8.84	0.15	7.11	0.09	1.17	0.04	0.14	
Au 5	75.60	10.51	8.89	1.03	1.96	0.52	0.80	0.07	0.64	
Au 6	74.01	12.78	11.44	0.24	0.56	0.03	0.81	0.02	0.12	
Au 7	74.24	13.62	11.29	0.02	0.19	0.02	0.63	0.00	0.00	
Au 8	74.07	13.13	12.00	0.03	0.07	0.04	0.55	0.05	0.06	
Au 9	73.25	14.82	7.76	0.26	2.12	0.16	1.46	0.04	0.13	
Au 10	72.19	13.75	8.76	0.00	2.32	0.00	2.84	0.00	0.14	
Au 11	70.88	16.31	7.27	0.03	2.17	0.73	1.99	0.03	0.59	
Au 12	73.42	15.31	9.36	0.14	0.43	0.13	1.10	0.01	0.11	

very similar to those of the associated Pd–As–Te PGM (Fig. 4C). In BSE images stillwaterite is only slightly less bright than the other Pd–As–Te minerals (Fig. 5B); therefore the mineral could be only identified by qualitative EDS analysis. Stillwaterite generally forms irregular patches or discontinuous rims along the vysotskite or the Pd–As–Te minerals, indicating replacement relationships (Figs. 4C-1, 5B). Usually, it exhibits bad polishing, rugged surface and a distinct porosity that in some cases is filled with an Fe oxide, probably magnetite. These paragenetic features suggest that stillwaterite in the Baranskoe-Kluevsky samples may have formed at relatively low temperature. Most compositions (Table 2) do not fit the theoretical stoichiometry Pd_8As_3, but show slight cation deficiency (Fig. 8). Calculation of ten analyses on the basis of 11 a.p.f.u., results in the average formula $(Pd_{7.69}Pt_{0.01}Ag_{0.04}Fe_{0.16}Cu_{0.05})_{7.95}(As_{3.02}S_{0.02}Te_{0.01})_{3.05}$. Thus, compared with compositions reported in the literature (*Cabri* et al., 1975; *Hänninen* et al., 1986; *Cabri*, 2002), the stillwaterite from Baranskoe-Kluevsky is distinctly different because of the lack of Sb and Bi, the very low Pt content, and the remarkable presence of Ag and base metals.

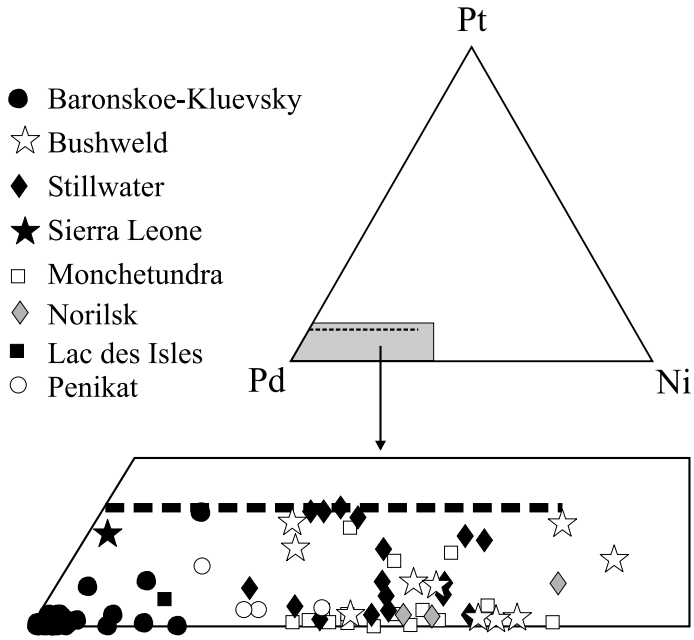

Fig. 7. Composition (at%) of vysotskite from Baranskoe-Kluevsky compared with those from Bushveld (*Verryn* and *Merkle*, 1994), Stillwater (*Cabri* et al., 1978; *Volborth* et al., 1986), Sierra Leone (*Bowles*, 2000), Monchetundra (*Grokhovskaya* et al., 2002), Noril'sk (*Genkin* and *Zvyagintsev*, 1962), Lac des Isles (*Cabri* et al., 1978), and Penikat (*Halkoaho*, 1989)

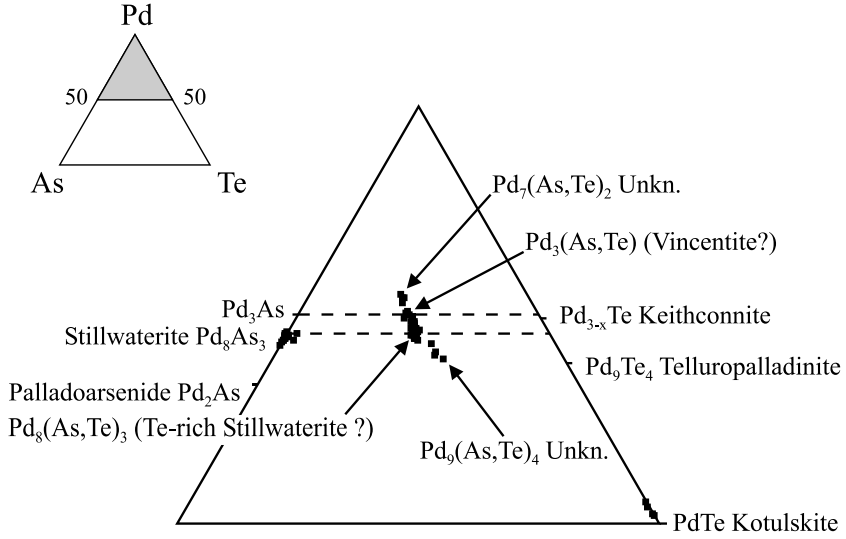

Fig. 8. Pd–As–Te compositions (at%) of stillwaterite, kotulskite and unknown Pd–arsenotellurides from Baranskoe-Kluevsky. The compounds $Pd_8(Te,As)_3$ and $Pd_3(Te,As)$ are ascribed to Te-rich stillwaterite and vincentite, respectively

The unknown Pd–As–Te minerals

These minerals are the second most abundant PGM species in the Baranskoe-Kluevsky samples. They form grains of 10 to 50 μm, generally confined to the external border of the sulfide blebs, replacing vystotskite and chalcopyrite (Figs. 4C, C-1, 5A, C, D). In some cases, they are replaced by stillwaterite (Fig. 5B). The arsenotellurides are characterized by very similar optical properties (creamy white color, weak anisotropy and reflectance) and brightness in BSE images (> vysotskite); therefore they could only be identified on the basis of qualitative EDS analysis by the consistent presence of Pd, As and Te peaks in variable proportions. The mineral chemical compositions (Table 2) plotted in the ternary diagram Pd–As–Te (Fig. 8), define a trend of Pd–Te substitution between the end members $Pd_7(As,Te)_2$ and $Pd_9(As,Te)_4$, with the As–Te ratio decreasing from 1.35 to 0.7. These minerals possibly represent new mineral species, however, two groups of compositions referable to the intermediate stoichiometries: $Pd_3(As,Te)$ and $Pd_8(As,Te)_3$, with As–Te ratios close to 1.0, may be ascribed to the Te-rich varieties of stillwaterite and vincentite, respectively.

$Pd_8(As,Te)_3$, possibly Te-rich stillwaterite

Repeated electron microprobe analyses of ten grains gave an almost constant composition corresponding to the average formula $(Pd_{7.79}Ag_{0.04}Fe_{0.11}Cu_{0.06}\ Ni_{0.01})_{8.00}(As_{1.52}Te_{1.46}S_{0.02})_{3.00}$, calculated on the basis of 11 a.p.f.u. The stoichiometry suggests that this mineral is stillwaterite, in which one half of the As has been substituted by Te and by some S (Fig. 8), possibly as a result of solid solution with telluropalladinite (Pd_9Te_4) or keithconnite ($Pd_{3-x}Te$). The substitution of As by Te has not been reported in stillwaterite from other localities, so far (*Cabri* et al., 1975). One grain showed slight enrichment in Ag (up to 0.22 a.p.f.u.), and decrease of the base metal content down to 0.03 a.p.f.u. (Fe + Cu + Ni), suggesting limited solid solution with the rare mineral telargpalite $(Pd_{2.8}Ag_{0.2})_3Te$ (*Kovalenker* et al., 1974).

$Pd_3(As,Te)$, possibly Te-rich vincentite

Microprobe analyses obtained on a number of grains gave the average composition $(Pd_{2.9}Fe_{0.06}Cu_{0.02})_{2.97}(As_{0.54}Te_{0.47})_{1.02}$ calculated on the basis of 4 a.p.f.u. This composition recalls that of arsenotellurides reported from two placer deposits in Ecuador and Madagascar, $(Pd_{2.93}Pt_{0.04}Cu_{0.04})_{3.01}(As_{0.51}Te_{0.48})_{0.99}$ and $(Pd_{2.69}Pt_{0.29}Fe_{0.1}Cu_{0.04})_{3.12}(As_{0.34}Te_{0.48}S_{0.06})_{0.88}$. The mineral was ascribed alternatively to an intermediate species between the discredited guanglinite Pd_3As (*Cabri*, 1980) and keithconnite $Pd_{3-x}Te$ (*Weiser* and *Schimdt-Thomé*, 1993), or to a Te-rich variety of vincentite (*Augé* and *Legendre*, 1992). Vincentite from the type locality in SE Borneo is monoclinic, characterized by a light brownish color, weak anisotropy, and a composition expressed by the formula $(Pd_{2.61}Pt_{0.37})_{2.99}(As_{0.44}Sb_{0.3}Te_{0.27})_{1.01}$ (*Stumpfl* and *Tarkian*, 1974; *Tarkian* et al., 2002). The unknown mineral from Kluevsky has optical properties similar to vincentite, and therefore attribution to a Sb-free Te-rich variety of vincentite (*Augé* and *Legendre*, 1992) is favored.

Electrum

Electrum is the main mineral carrier of gold. It occurs as small inclusions (<40 μm) in vysotskite, chalcopyrite (Figs. 4C, C-1, 5A, B, C) or in the secondary magnetite, but it has never been observed inside the Pd–Te–As minerals. The inclusions in vysotskite and chalcopyrite frequently have drop-like or vermicular shape, suggesting an origin by subsolidus exsolution (Fig. 6A, B, C). The association with magnetite does not reflect equilibrium conditions, since the oxide clearly represents a late replacement of chalcopyrite. Repeated analyses of several grains of electrum (Table 3) revealed relatively constant proportions of Au (69.1–75.6 at%) and Ag (16.3–10.4 at%) with high contents of Pd (7.0–12.0 at%), accompanied by minor amounts of Pt (0.25–1.03 at%) and base metals (0.7–8.4 at% Fe + Cu + Ni).

Interpretation of the paragenesis

The BSE study of the internal texture of the sulfide blebs indicates that the ore mineral assemblage formed by a sequence of crystallization events. At least three successive stages can be distinguished. The first stage was characterized by formation of the vysotskite–chalcopyrite–kotulskite–electrum assemblage. Vysotskite and chalcopyrite crystallized together, and were closely followed by exsolution of kotulskite from vysotskite and electrum from both vysotskite and chalcopyrite. The whole assemblage indicates that the ore initially was in the stability field of a sulfide phase predominantly composed of Cu–Pd–Au–Ag with minor amounts of Pt and Te. The marginal position of the arsenotellurides and kotulskite in the sulfide blebs suggests that the suite of Pd–As–Te–(Ag) minerals crystallized in a subsequent step, replacing former vysotskite and, in some cases, chalcopyrite. Sulfur, Au and Pt did not take part in this stage of ore formation, whereas the system was dominated by Te and As. In the last step, Te activity decreased and the system became enriched in As, leading to the formation of stillwaterite that generally overgrows or replaces the arsenotellurides.

The sequence of crystallizing phases reflects important chemical changes with decreasing temperature in the ore forming system. From an initial stage characterized by relatively high S fugacity, the system became enriched in Te–As, and finally evolved to a late As-dominated stage. The textures suggest that the early crystallized Cu–Pd sulfides were not in equilibrium with the later Te–As rich fluid. They reacted and were partly replaced by a new assemblage containing rare Pd arsenotellurides. The occurrence of stillwaterite–magnetite intergrowths suggest that the final As-dominated stage was closely followed by magnetite replacement. In all the examined samples, magnetite has the textural characteristics of a secondary phase. Its formation is probably related with the serpentine–chlorite alteration of the silicates, indicating substantial increase of water activity and the establishment of oxidizing conditions typical of a sub-critical hydrothermal solution. It is difficult to establish if the crystallization of magnetite is a late distinct episode unrelated to mineralization, or represents the final stage of the mineralization. In any case, it does not appear to have affected the PGM–Au assemblage, but only resulted the oxidation of the base metal sulfides.

Concluding remarks

1) The results presented in this study confirm that the high Au + Pd concentrations in the drill cores at the level of several g/t are accounted for by a complex assemblage of precious Au and Pd minerals associated with disseminated chalcopyrite–magnetite blebs. The precious metal assemblage includes Pd-rich electrum, vysotskite, kotulskite, the rare mineral stillwaterite, and a series of unknown compounds in the Pd–As–Te ternary system, two of which are tentatively attributable to the Te-rich varieties of stillwaterite and vincentite. Alternatively, these compounds may represent a group of new phases, having limited solid solution between the two end members $Pd_9(As,Te)_4$ and $Pd_7(As,Te)_2$, at As–Te ratios close to 1.0 in the Pd–As–Te ternary system (Fig. 7). Structural investigation is needed to clarify this question.
2) The mineralogical data and paragenetic observations presented in this paper indicate that the Kluevsky Pd–Au mineralization hosted in the serpentinized apatite-rich olivinite did not form in a pure magmatic system. The Cu-rich nature of the sulfide blebs is inconsistent with the composition of natural magmatic sulfide liquids that generally lies in the Fe-rich field of the Fe–Ni–Cu ternary system. There is neither mineralogical nor geochemical evidence that pyrrhotite and pentlandite ever existed in the blebs prior to magnetite replacement. No relics or alteration products of these base metal sulfides have been encountered and, notably, none of the analyzed ore minerals contains Ni in appreciable concentrations. In particular, the Ni-poor composition of the Baranskoe-Kluevsky vysotskite compared with vysotskite from major layered intrusions suggests crystallization of the mineral at relatively low temperature with respect to magmatic thermal conditions (*Makovicky* and *Karup-Moller*, 1995; *Verryn* and *Merkle*, 1994, 2000). Experimental studies indicate that the absence of Ni and the enrichment in Cu, Pd and Au are distinctive features of PGE deposits formed under high activity of fluids, compared with those formed by sulfide liquid segregation in pure magmatic systems (*Ballhaus* et al., 1994). Consistently, the Pd–Au deposits of the Volkovsky-type are believed to have formed in the temperature range of 600–400 °C, in a geological environment characterized by high fluid activity and oxygen fugacity (*Volchenko* and *Koroteev*, 1998). The data presented in this paper apparently confirm this hypothesis and indicate that the PGM assemblage formed by the action of fluids in which the fugacity of S decreased and that of Te and As increased with decreasing temperature. The origin of the mineralizing fluid phase in the Volkovsky-type deposits (residual post-magmatic hydrous fluids or hydrothermal solutions from an external source) remains an open question.

Acknowledgements

Financial support of the RFBR (Russian Foundation of Basic Research, grant 04-05-96009-r2004ural) to the Russian co-authors is gratefully acknowledged. Thanks are also due to the Italian Ministry of Education, University and Research (MIUR), COFIN 2001, leader *C. Cipriani*. The authors are grateful to the Editors *E. F. Stumpfl* and *J. G. Raith* and to *M. Tarkian* and an unknown referee for their useful suggestions.

References

Anderson WB, Martineau MP (2002) New discoveries of platinum and palladium in the central Urals of Russia. In: *Boudreau A* (ed) Abtracts, Ninth International Platinum Symposium, Billings, Montana, USA, pp 9–12

Augé T, Legendre O (1992) Pt–Fe nuggets from alluvial deposits in eastern Madagascar. Can Mineral 30: 983–1004

Ballhaus CG, Ryan CG, Mernagh TP, Green DH (1994) The partitioning of Fe, Ni, Cu, Pt and Au between sulphide, metal and fluid phases: a pilot study. Geochim Cosmochim Acta 58: 811–826

Barkov AY, Martin RF, Halkoaho TAA, Criddle AJ (2002) Laflammeite, $Pd_3Pb_2S_2$, a new platinum-group mineral species from the Penikat layered complex, Finland. Can Mineral 40: 671–678

Bowles JFW (2000) Prassoite, vysotskite and keithconnite from the Freetown layered complex, Sierra Leone. Mineral Petrol 68: 75–84

Cabri LJ (1980) New mineral names. Am Mineral 63: 184

Cabri LJ (2002) The Platinum-Group minerals. Can Inst Mining Metallurg Petrol Spec Vol 54: 13–129

Cabri LJ, Laflamme JHG (1974) Rhodium, platinum and gold alloys from the Stillwater complex. Can Mineral 12: 399–403

Cabri LJ, Laflamme JHG, Stewart JM, Rowland JF, Chen TT (1975) New data on some palladium arsenides and antimonides. Can Mineral 13: 321–335

Cabri LJ, Laflamme JHG, Stewart JM, Turner K, Skinner BJ (1978) On cooperite, braggite and vysotskite. Am Mineral 65: 832–839

Criddle AJ, Stanley CJ (1985) Characteristic optical data for cooperite, braggite and vysotskite. Can Mineral 23: 149–162

Donovan JJ, Rivers ML (1990) PRSUPR-A PC based automation and analyses software package for wavelength dispersive electron beam microanalysis. Microbeam Anal: 66–68

Genkin AD, Zvyagintsev OE (1962) Vysotskite, a new sulfide of palladium and nickel. Zapiski Vses Mineral Obshch 91: 718–725 (in Russian)

Grokhovskaya TL, Bakaev GF, Lapina M (2002) PGE mineralization in the Paleoproterozoic Manchetundra layered igneous complex (the Baltic shield, Russia). In: *Boudreau A* (ed) Abtracts, Ninth International Platinum Symposium, Billings, Montana, USA, pp 161–164

Halkoaho T (1989) Ala-Penikat platinametallimineralissatiot Penikkain kerrosintruusiossa. Raporti n. 2, Perapohjan platinaprojekti, Olulun Yliopisto, 173 pp (in Finnish)

Hänninen E, Törnroos R, Seppo IL (1986) Stillwaterite and associated platinum group minerals from the Siikakämä layered mafic intrusion, northern Finland. Lithos 19: 87–93

Ivanov OK (1997) Concentrically-zoned pyroxenite dunite massifs of the Urals. Ural State University, Ekaterinburg, 488 pp (in Russian)

Kovalenker VA, Genkin AD, Evstigneeva TL, Laputina IP (1974) Telargapalite, a new mineral of palladium, silver and tellurium from the copper–nickel ores of the Oktyabr deposit. Zapiski Vses Mineral Obshch 103: 595–600 (in Russian)

Makovicky E, Karup-Moller S (1995) The system Pd–Fe–Ni–S at 900 and 725 °C. Mineral Mag 59: 685–702

Murzin VV, Moloshag VP, Volchenko YuA (1988) Paragenesis of the noble metal minerals in cooper–iron–vanadium ores of the Volkovka-type in the Urals. Dokl Akad Nauk 300: 1200–1202 (in Russian)

Potter M (2002) Palladium soil geochemistry, Barabskoye Pd–Au prospect, Sverdlovsk oblast, Russia. Trans Inst Mineral Metall Sect B Appl Earth Sci 111: 58–64

Stumpfl EF, Tarkian M (1974) Vincentite, a new palladium mineral from south-east Borneo. Mineral Mag 39: 525–527

Tarkian M, Klaska KH, Stumpfl EF (2002) New data on vincentite. Can Mineral 40: 457–461

Tood SG, Keith DW, Le Roy LW, Schissel DJ, Mann EL, Irvine TN (1982) The J–M platinum–palladium reef of the Stillwater Complex, Montana. Econ Geol 77: 1454–1480

Verryn SMC, Merkle RKW (1994) Compositional variation of cooperite, braggite, and vysotskite from the Bushveld Complex. Mineral Mag 58: 223–234

Verryn SMC, Merkle RKW (2000) Synthetic ''Cooperite'', ''Braggite'', and ''Vysotskite'' in the system PtS–PdS–NiS at 1100 °C, 1000 °C, and 900 °C. Mineral Petrol 68: 63–73

Volborth A, Tarkian M, Stumpfl EF, Housley RM (1986) A survey of Pd–Pt mineralization along the 35 km strike of the J–M reef, Stillwater complex, Montana. Can Mineral 24: 329–346

Volchenko YuA, Koroteev V (1998) The Urals platinum: new type of mineralization. In: *South African Institute of Mining and Metallurgy* (ed) Eighth International Platinum Symposium. Abstracts, Symposium Series S18: 435–437

Volchenko YuA, Necheukhin VM, Padigin AI, Sandler GA (1975) New type of platinum mineralization in ultramafites of the folded belts. Dokl Akad Nauk 224: 182–189 (in Russian)

Weiser T, Schimdt-Thomé M (1993) Platinum-group minerals from the Santiago River, Esmeraldas Province, Ecuador. Can Mineral 31: 61–73

Yefimov AA, Yefimova LP, Maegov VI (1993) The tectonics of the Platinum-bearing belt of the Urals: composition and mechanism of structural developments. Geotectonics 27: 197–207

Zoloev KK, Volchenko YuA, Koroteev VA, Malakhov IA, Mardirosyan AN, Khripov VN (2001) Platinum ores in different complexes of the Urals. Ural State University Press, Ekaterinburg, 199 pp (in Russian)

Authors' addresses: *F. Zaccarini*, Department of Applied Geosciences and Geophysics, University of Leoben, Peter-Tunner-Strasse 5, A-8700 Leoben, Austria, e-mail: fedezac@tsc4.com; *E. Anikina, E. Pushkarev*, and *I. Rusin*, Institute of Geology and Geochemistry, Ural-Branch of the Russian Academy of Sciences, Str. Pochtovy per. 7, 620151 Ekaterinburg, Russia; *G. Garuti*, Dipartimento di Scienze della Terra, Università degli Studi di Modena e Reggio Emilia, Via S. Eufemia, 19, 41100 Modena, Italy